Sequence Effects in Bicycle Routes: Exploratory Evidence from GPS Cycling Trajectories

Victoria Dahmen

Ayda Grisiute

Martin Raubal

Klaus Bogenberger

STRC Conference Paper 2026 **May 21, 2026**

STRC | **26th Swiss Transport Research Conference**
Monte Verità / Ascona, May 20-22, 2026

Sequence Effects in Bicycle Routes: Exploratory Evidence from GPS Cycling Trajectories

Victoria Dahmen
Chair of Traffic Engineering & Control
Technical University of Munich
v.dahmen@tum.de

Ayda Grisiute
Institute of Cartography and Geoinformation
ETH Zurich, Zurich, Switzerland
agrisiute@ethz.ch

Martin Raubal
Institute of Cartography and Geoinformation
ETH Zurich, Zurich, Switzerland
mraubal@ethz.ch

Klaus Bogenberger
Chair of Traffic Engineering & Control
Technical University of Munich
klaus.bogenberger@tum.de

May 21, 2026

Abstract

As cycling is actively promoted and cities aim to improve cycling infrastructure, safety, and comfort, it is not only relevant which routes cyclists take, but also where along those routes they would most value improvements. The success of such measures ultimately hinges on human factors, such as perception and cognitive biases. Bicycle route choice has been studied extensively, yet sequence effects, i.e., the order in which spatial properties are encountered along a route, have received little attention so far. As recent work has suggested their relevance, in this study we utilize bicycle trajectory data from Zurich and Munich to investigate whether such sequence effects observed in a controlled lab experiment are also present in real-world data. We consider different route segmentation strategies to derive meaningful sequences. By assessing route deviations from the shortest routes, we uncover the cyclists' bias towards specific segment sequences. The experimental patterns are present to varying extents in real-world cycling trajectories. The observed behavioral patterns can be leveraged to support planning policies for allocating road space to bike lanes where their position along common routes improves the cycling experience the most, or to enhance experiential bicycle routing.

Keywords

GPS-traces; routing behavior; cognitive bias; route segmentation; cycling.

Preferred citation

Dahmen, V., Grisiute A., Raubal M., and Bogenberger R. (2026) Sequence Effects in Bicycle Routes: Evidence from GPS Cycling Trajectories, paper presented at the *26th Swiss Transport Research Conference (STRC 2026)*, Ascona, May 2026.

Contents

List of Tables

List of Figures

1 Introduction

In recent years, cycling has seen a resurgence due to its positive externalities, such as reduced emissions, lower space consumption, and health benefits (Oja *et al.*, 2011). To effectively promote cycling and encourage a sustainable modal shift, it is crucial to understand how cyclists perceive their journeys, including the cognitive biases that shape long-term travel behavior (Adam, 2026; Willis *et al.*, 2015).

While many route cost models successfully integrate segment-level features (e.g., infrastructure quality, traffic exposure) and user demographics (e.g., car ownership) (Meister *et al.*, 2023), they largely overlook the episodic spatial structure of the cycling experience. Key psychological factors, such as sequence effects (e.g., the peak-end rule), are frequently excluded (Skov-Petersen *et al.*, 2018; Teimouri *et al.*, 2023). Furthermore, large-scale, real-world analyses validating these lab-based phenomena remain scarce.

Therefore, it is of interest to explore whether these sequence effects manifest in real-world cycling behavior. If perceptions are sensitive to temporal ordering, two routes with identical objective characteristics (but ordered differently) could produce systematically different experiences (Abenoza *et al.*, 2019). This has direct implications for routing and mobility models trained on GPS trajectories, which implicitly absorb these cognitive biases. Advancing toward human-centered AI systems requires shifting from this implicit absorption to the explicit modeling of cognitive mechanisms (Pappalardo *et al.*, 2023).

In this exploratory paper, we investigate whether sequence effects observed in a controlled lab setting (Grisiute *et al.*, in preparation) are detectable in real-world GPS cycling trajectories from Munich and Zurich. We partition observed routes and their shortest-path counterparts into positional segments using five segmentation strategies as proxies for the cognitive abstraction of routes, and compare them through two complementary metrics: a *learned cost* and *path dissimilarity*.

2 Cognitive Biases in Cyclist Behavior

Cyclists do not always select routes based on shortest distance or travel time (Krenn *et al.*, 2014; Park and Akar, 2019). Instead, their choices are shaped by cognitive heuristics, such as minimizing turns, avoiding complex intersections, or maintaining a direct heading,

which cause observed behavior to deviate from normative, utility-maximizing routing models (Wiener *et al.*, 2008; Teimouri *et al.*, 2023). While higher cognitive load during spatial decision-making increases reliance on these heuristics (Brunyé *et al.*, 2018), existing empirical studies remain scarce (Abenoza *et al.*, 2019). In particular, sequence effects, i.e., the order in which spatial properties are encountered, remain largely unexplored outside of lab experiments (Grisiute *et al.*, in preparation), motivating large-scale, data-driven empirical investigation using GPS cycling trajectories. Trajectory mining allows identifying recurring heuristic travel behavior at scale (Zheng, 2015). Other biases, including last-mile effects and preferences for common paths, are also detectable (Teimouri *et al.*, 2023). Revealing them generally requires spatial abstraction, such as trajectory segmentation, clustering decision points, or identifying route-defining locations (Teimouri and Richter, 2022, 2025; Sultan *et al.*, 2017; Griesbauer *et al.*, 2024; Manley *et al.*, 2015; Grisiute and Raubal, 2024). This suggests that observed cycling biases are closely linked to how routes are cognitively planned and decomposed, rather than to segment-level optimization alone.

Controlled lab experiment. Initial evidence for sequence effects in cycling was established in a controlled lab setting (Grisiute *et al.*, in preparation). Participants ($N = 60$) evaluated composite video routes assembled from three 30-second segments of dominantly positive or negative cycling quality from Zurich streets. Varying the positional placement of a single contrasting segment revealed that the temporal arrangement of route features affects overall reported experience, serving as the primary motivation for our data-driven exploratory study.

3 Methodology

Our exploratory analysis follows a three-stage workflow: (i) defining the spatial hierarchy of the analysis units, (ii) applying trajectory segmentation based on cognitive and geometric strategies, and (iii) calculating two comparative metrics between derived segments of observed trajectories and their shortest-path benchmarks.

Defining key elements. To analyze sequence effects, we first define a nested structure of spatial units, moving from the macro-level trajectory traces down to the micro-level street edge. **Trajectory (P):** Let $G = (V, E)$ be the street network graph. A trajectory

$P = (e_1, \ldots, e_m)$ is an ordered sequence of edges $e_i \in E$ connecting an origin-destination (OD) pair. We compare each *observed trajectory* (P^{obs}) from the Munich and Zurich datasets against its distance-based *shortest path* (P^{sp}). **Segment (s):** Each trajectory is partitioned into N segments via a segmentation strategy $S(P) = \{s_1, s_2, \ldots, s_N\}$, where each s_k is a contiguous sub-sequence of P and their concatenation recovers P. These segments allow for a localized analysis of travel cost and behavior across different stages of a journey and typically vary in length. In this study, we fix $N = 3$, inspired by the lab experiment design, and refer to the segments as *start*, *middle*, and *end*. Segmentation strategies are described in more detail in Section 3.1. **Edge (e):** The atomic unit of the street network, which is associated with specific attributes (e.g. length, infrastructure type) and a cost.

3.1 Trajectory Segmentation Strategies

To assess sequence effects, we apply five segmentation strategies (Zheng, 2015) to partition P^{obs} and P^{sp} into $N = 3$ segments, varying in their degree of cognitive modeling. **Equal Distance** serves as a cognitively neutral baseline, dividing trajectory length L into three equal segments of $L/3$ at the nearest vertex. **Homogeneity Boundary** places split points where edge costs change most drastically (Buchin *et al.*, 2011), assuming significant cost shifts trigger salient perceptual transitions. **Spatial Simplification** split points are vertices with maximum perpendicular deviation from the origin-destination straight line based on the Douglas-Peucker algorithm (Douglas and Peucker, 1973). **Salient Heading Changes** treats the largest angular deviations between consecutive edges as natural cognitive boundaries (Zheng, 2015). Finally, **Attribute Embedding** represents each edge as a multi-dimensional feature vector (e.g., speed limits, lanes) (Skupin, 2008), placing split points where Euclidean distances between adjacent embeddings are maximized.

3.2 Metrics for Comparative Analysis

We evaluate the cycling attractiveness and characteristics of the segments of the observed trajectories P^{obs} and shortest routes P^{sp} using two complementary metrics to quantify the deviation between these. These two metrics are presented in more detail below.

Metric 1: Learned Cost. This metric represents the perceived route cost, learned from

the Munich trajectory dataset. Initially, an optimization framework determined edge costs that minimized the gap between observed routes and distance-weighted shortest paths. Subsequently, a neural network was trained to predict these costs based on edge-level attributes (Dahmen *et al.*, 2025). Table 2 elaborates on these attributes. As this length-independent learned cost encapsulates cyclists' preferences for different street edge characteristics, we use it to evaluate the attractiveness of each segment s_k. We define a segment's length-weighted mean cost $\bar{c}(s_k)$ and the segment-wise cost difference $\Delta\bar{c}_k$:

$$\Delta\bar{c}_k = \bar{c}(s_k^{\text{sp}}) - \bar{c}(s_k^{\text{obs}}), \quad \text{where} \quad k \in \{1,2,3\} \quad \text{and} \quad \bar{c}(s_k) = \frac{\sum_{e\in s_k} \ell_e\, \hat{c}_e}{\sum_{e\in s_k} \ell_e}, \tag{1}$$

where ℓ_e is the length of edge e and $\hat{c}_e$ is its learned cost. A positive $\Delta\bar{c}_k$ indicates that the observed segment traverses edges of lower perceived cost than its shortest-path equivalent, and vice versa.

Metric 2: Path dissimilarity. This metric serves as a general, location-agnostic complement to the learned cost metric, capturing the physical and environmental differences between segment pairs. It calculates the Euclidean distance between segment-level attribute vectors. We utilize the same set of edge attributes (Table 2), augmented with angularity. All attributes are min-max normalized across all network edges prior to aggregation. For each segment s_k^r, where $r \in \{\text{obs}, \text{sp}\}$, we compute the length-weighted average of the normalized edge attributes $\tilde{x}_{j,e}$ to form a segment-level vector $\bar{\tilde{\mathbf{x}}}_k^r = (\bar{\tilde{x}}_{k,1}^r, \ldots, \bar{\tilde{x}}_{k,J}^r)$. The segment-wise dissimilarity Δd_k is then computed as:

$$\Delta d_k = \left\| \bar{\tilde{\mathbf{x}}}_k^{\text{sp}} - \bar{\tilde{\mathbf{x}}}_k^{\text{obs}} \right\|_2, \quad \text{where} \quad k \in \{1,2,3\} \quad \text{and} \quad \bar{\tilde{x}}_{k,j} = \frac{\sum_{e\in s_k} \ell_e\, \tilde{x}_{j,e}}{\sum_{e\in s_k} \ell_e}, \tag{2}$$

where a larger Δd_k indicates greater dissimilarity in road environment character between the observed and shortest-path segment.

Testing the hypothesis. To determine if sequence effects influence cycling behavior, we compare the segment-level metrics of the first segment ($k = 1$) against the final segment ($k = 3$) derived from all trajectory pairs (P^{obs} and P^{sp}). We focus on start and end segments because both are geographically anchored by the origin and destination, providing comparable spatial constraints. We perform paired t-tests independently for both evaluation metrics: learned cost ($\Delta\bar{c}_k$) and path dissimilarity (Δd_k). We test the null hypothesis (H_0) that there is no difference in the mean deviation between the start and end of a trajectory for either metric. A statistically significant result would show that temporal position plays a detectable role in route choice.

3.3 Case Study and Data Preprocessing

We apply our methodology to bicycle and e-bike trajectories from two app-based GPS studies: Munich's *Mobilität.Leben* (Loder *et al.*, 2024) (May 2022–Dec 2023), which generated travel diaries via automated mode-detection, and a Zurich-focused subset of a 2017 *SBB Green Class* study (Martin *et al.*, 2019) on Mobility-as-a-Service in Switzerland.

Trajectory Preprocessing. We map-match trajectories from both datasets to their respective street networks and apply targeted filters. These include removal of with insufficient GPS precision, map-matched deviations exceeding 50 m (150 m at start/end points), and round trips. We further restrict trajectories to be fully contained within the study area, capping speeds at 28 km/h (99th percentile), enforcing a 3-minute minimum duration, and a 5 km maximum length to harmonize datasets (maximum length in the Munich dataset). This yields 452 paths (24 users) in Zurich and 1,000 paths (244 users) in Munich. For downstream tasks, we identify repeat trips (paths sharing $\geq$90 % of edges or differing by $\leq$3 edges).

Network Preprocessing. We prepare the street network using *OSMNetFusion* (Dahmen, 2025), which retrieves OpenStreetMap data for a specific date, simplifies topology while retaining tags, and appends open elevation and land-use data. Missing attributes are addressed by supplementing Munich with cycle path widths (Landeshauptstadt München, 2019) and Zurich with 2021 open data (Zürich, 2021). Network topology, morphology, and cycling infrastructure differ notably between the two cities (Table 2). The learned cost is, on average, higher for Zurich (7.6) than Munich (6.6), with a distribution showing more costly edges in Zurich (Figure 2). Munich is flatter with wider roads and predominantly one-directional cycle paths, while Zurich is hillier and, in 2017, offered little dedicated bicycle infrastructure.

4 Results

To investigate whether sequence-dependent routing patterns manifest in real-world trajectories, we systematically compare the first ($s_{k=1}$) and last ($s_{k=3}$) segments of observed trajectories across the Munich and Zurich datasets. We focus on these segments because both are constrained by origin-destination, whereas the middle segment ($s_{k=2}$) affords

the greatest routing flexibility. Since cognitive boundaries are inherently subjective, we evaluate our two metrics (learned cost $\Delta\bar{c}_k$ and path dissimilarity Δd_k) across five segmentation strategies (see Section 3.1).

Metric Relations Across Datasets. Since both metrics draw on largely the same edge attributes, we first establish their relationship. For Munich, absolute cost difference and path dissimilarity exhibit a strong correlation ($R^2 = 0.43$), confirming they capture related but distinct aspects of spatial deviation. The correlation is similar for Zurich ($R^2 = 0.48$), despite its smaller sample size and the fact that the learned cost model was trained on Munich data. Importantly, the learned cost carries a sign, indicating whether the observed route is better or worse than the shortest path. Path dissimilarity is a non-negative scalar measuring absolute Euclidean deviation. For Munich, the mean absolute learned cost difference ($|\Delta\bar{c}_3| = 0.18$) is lower than that of Zurich ($|\Delta\bar{c}_3| = 0.22$), while the mean path dissimilarity is higher for Munich ($\Delta d_3 = 0.54$) than for Zurich ($\Delta d_3 = 0.40$).

Learned Cost. If cyclists disproportionately improve the final portion of their journey, we expect $\Delta\bar{c}_1 - \Delta\bar{c}_3 > 0$. As shown by the paired t-tests in Figure 1, this is observed for about half of all cases in Munich, but rarely for Zurich. In Table 1, values below/above the 2.5th/97.5th percentile are not considered. When considering all paths, the 3rd segment in Munich and Zurich shows improvement under only one of the segmentation strategies. The magnitude of this improvement is marginal, underscoring the metric's sensitivity to both the segmentation strategy and the city-specific cost model.

Path Dissimilarity. For Δd_k, higher values indicate greater deviation from the shortest path. The middle segment ($s_{k=2}$) consistently shows the highest absolute deviation, reflecting the unconstrained routing freedom. When comparing the OD-constrained segments, the mean difference ($\Delta d_1 - \Delta d_3$) is negative in most configurations (Table 1), indicating that the latter segment is improved more, though standard deviations remain large relative to the effect size. Significance is observed primarily under the *Attribute Embedding* and *Equal Distance* strategies (Figure 1).

Moderating Factors. Given the high aggregate variance, we subset trajectories to isolate key behavioral moderators (Figure 1). For short trips (1–2 km), the final segment is improved significantly more than the first across nearly all segmentation strategies in both cities for the path dissimilarity. This effect diminishes with trip length, likely due to the compounding cognitive demands of longer route planning. For the learned cost, this effect is reversed. Familiarity also moderates the effect: repeatedly performed trips (where cyclists have iteratively refined their routes) show greater final-segment improvement

in more cases than for unfamiliar routes for the learned cost metric, but not for path dissimilarity. Finally, trip purpose plays a role too: sequence-dependent improvements are more pronounced in work commutes than in leisure trips for the learned cost in both regions. For the path dissimilarity, no substantial difference is observed for trip purpose.

Table 1: Comparison of mean and standard deviation differences for Zurich and Munich. Bold values indicate that segment 3 was improved more compared to segment 1.

Metric	Segmentation strategy	Zurich		Munich	
		mean	std	mean	std
$\Delta\bar{c}_1 - \Delta\bar{c}_3$	Attribute embedding	-0.109**	0.677	**0.001**	0.456
	Equal distance	-0.083**	0.463	-0.011	0.357
	Homogeneity boundary	-0.049*	0.486	-0.012	0.389
	Salient turns	**0.004**	0.606	-0.031*	0.456
	Spatial simplification	-0.066**	0.531	-0.013	0.395
$\Delta d_1 - \Delta d_3$	Attribute embedding	0.061*	0.555	**-0.050***	0.693
	Equal distance	**-0.051***	0.478	**-0.040***	0.561
	Homogeneity boundary	**-0.002**	0.514	**-0.03**	0.591
	Salient turns	**-0.006**	0.539	**-0.04**	0.694
	Spatial simplification	**-0.023**	0.471	**-0.029**	0.61

5 Discussion and Conclusion

This study offers an initial large-scale empirical test of whether sequence-dependent routing patterns, previously observed only in a controlled lab setting (Grisiute *et al.*, in preparation), are detectable in cycling trajectories. Through a dual-metric framework combining learned costs and attribute embeddings, we find that cyclists tend to deviate more from the shortest path in the final segment than the first. While statistically significant under several segmentation strategies, this pattern remains modest relative to overall path variance. This work should read as a first empirical probe: establishing the phenomenon's real-world presence, mapping the conditions under which it emerges, and surfacing the methodological challenges detailed below.

Our analysis reveals two methodological challenges and one unexpected finding. Regarding segmentation, the effect emerges under most, but not all, strategies. While equal distance and attribute embedding perform best, the lack of a single dominant strategy suggests the

Figure 1: Overview of whether the expected difference is observed between segment 1 and 3, and whether it is significant (t-test) - for various segmentation strategies and filters.

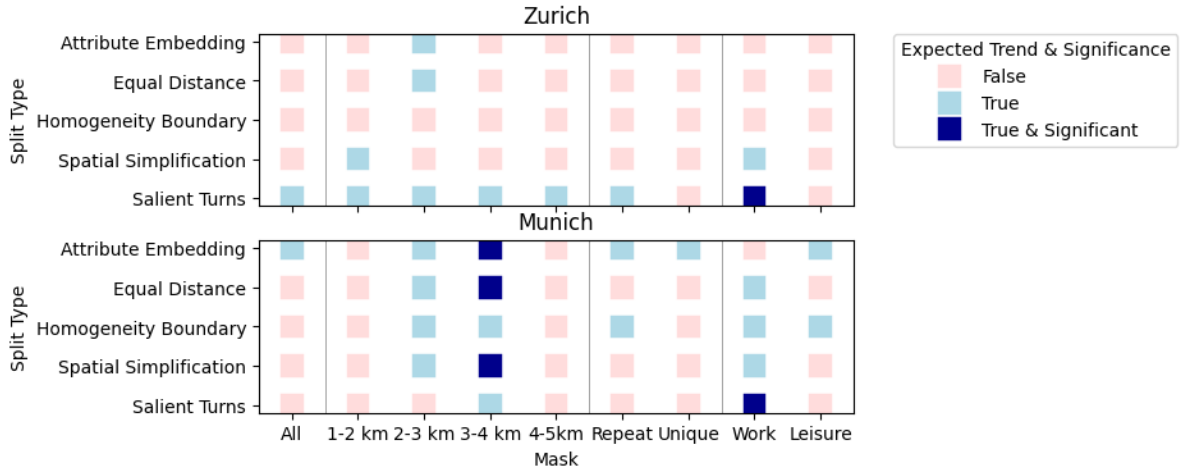

(a) **Metric 1: Learned Cost.** If the mean path-level learned cost difference ($\Delta\bar{c}_1 - \Delta\bar{c}_3$) is positive, the third segment is improved more than the first segment.

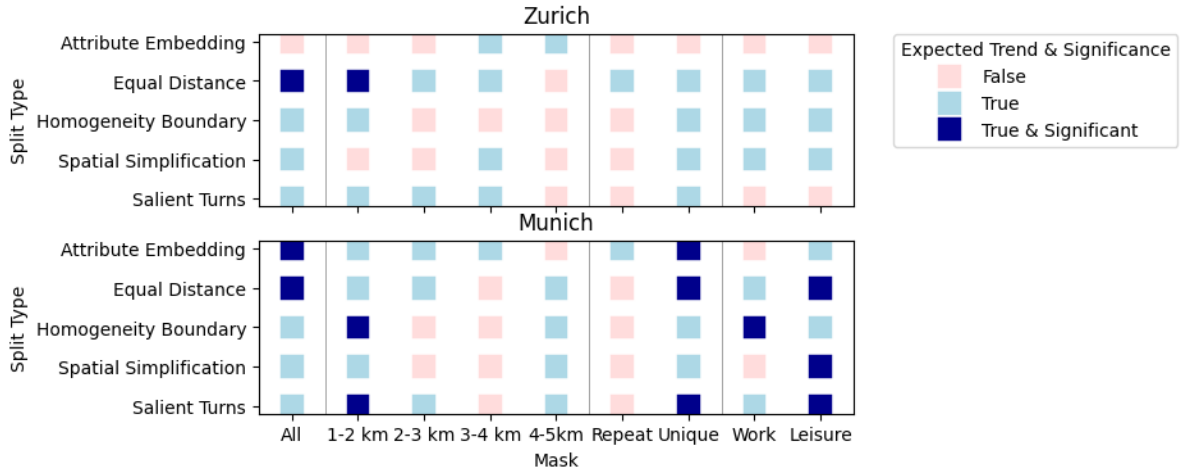

(b) **Metric 2: Path Dissimilarity.** If the mean path-level dissimilarity ($\Delta d_1 - \Delta d_3$) is negative, the third segment differs more from the shortest path than the first segment does.

effect is resilient to how routes are segmented. Regarding the two metrics, learned cost and path dissimilarity occasionally disagree due to their complementary designs. Learned cost captures directional preference (whether a route improves or degrades upon the shortest path), while path dissimilarity measures only the city-agnostic magnitude of deviation. This emphasizes the need for a unified, transferable, and directionally informative metric. Perhaps most intriguingly, the middle segment consistently exhibits the highest absolute deviation from the shortest path across both cities and metrics, which was not observed in the lab experiment. This likely reflects freedom from origin-destination anchoring, but whether this is a structural artifact or a cognitive phenomenon that spills into end-of-trip

perception remains an open question.

Several limitations present future work directions. Heterogeneity in data quality, demographics, and temporal coverage limits cross-city comparability, prompting further testing on additional datasets. The Munich-trained cost model may not transfer cleanly to Zurich, requiring city-agnostic or jointly trained alternatives. Because cognitive segmentation boundaries vary by individual and trip familiarity, moving away from group-level approximations to individual-based segmentation is a natural next step. Finally, fixing $N = 3$ is motivated by the lab design but may be insufficient for longer routes, which motivates follow-up experiments exploring the effect of sequence length.

Despite their exploratory nature, these findings point to two practical applications. First, navigation engines could optimize experiential trajectories rather than simply minimizing total cost. Second, explicitly modeling sequence structures would improve the behavioral validity of current route-choice models, as they may conflate attractive links with their positions. At the network scale, a "directional asymmetry" prevents naive unidirectional optimization and complicates potential interventions. Ultimately, demonstrating detectable sequence effects in naturalistic routing bridges cognitive lab findings with large-scale urban mobility data. Advancing this frontier requires developing more comprehensive metrics, individualizing segmentation strategies, and testing varied sequence lengths.

6 Acknowledgements

Victoria Dahmen acknowledges funding by the TUM Georg Nemetschek Institute Artificial Intelligence for the Built World.

7 References

Abenoza, R. F., O. Cats and Y. O. Susilo (2019) How does travel satisfaction sum up? An exploratory analysis in decomposing the door-to-door experience for multimodal trips, *Transportation*, **46** (5) 1615–1642, ISSN 0049-4488, 1572-9435.

Adam, C. (2026) A survey to measure cognitive biases in mobility choices and responses to urban policy, *Transport Policy*, **179**, 103988, ISSN 0967070X.

Brunyé, T. T., S. B. Martis and H. A. Taylor (2018) Cognitive load during route selection increases reliance on spatial heuristics, *Quarterly Journal of Experimental Psychology*, **71** (5) 1045–1056, May 2018, ISSN 1747-0218, 1747-0226.

Buchin, M., A. Driemel, M. Van Kreveld and V. Sacristan (2011) Segmenting trajectories: A framework and algorithms using spatiotemporal criteria, *Journal of Spatial Information Science*, (3) 33–63, ISSN 1948-660X.

Dahmen, V. (2025) OSMNetFusion: A Topologically Simplified Multimodal Information-Rich OSM Network (v1.0.0), `https://doi.org/10.5281/zenodo.17485919`.

Dahmen, V., A. Loder and K. Bogenberger (2025) A novel machine-learning, multi-criteria, centralized, bicycle routing algorithm, paper presented at the *104th Annual Meeting of the Transportation Research Board (TRB 2025)*.

Douglas, D. H. and T. K. Peucker (1973) ALGORITHMS FOR THE REDUCTION OF THE NUMBER OF POINTS REQUIRED TO REPRESENT A DIGITIZED LINE OR ITS CARICATURE, *Cartographica*, **10** (2) 112–122, ISSN 0317-7173, 1911-9925.

Griesbauer, E.-M., P. Fernandez Velasco, A. Coutrot, J. M. Wiener, J. G. Morley, D. McNamee, E. Manley and H. J. Spiers (2024) London taxi drivers exploit neighbourhood boundaries for hierarchical route planning, `http://biorxiv.org/lookup/doi/10.1101/2024.02.20.581139`.

Grisiute, A., P. Mavros and M. Raubal (in preparation) Sequence matters? understanding cognitive biases in subjective cycling experience, manuscript in preparation.

Grisiute, A. and M. Raubal (2024) Spatial Nudging: Converging Persuasive Technologies, Spatial Design, and Behavioral Theories, *LIPIcs, Volume 315, COSIT 2024*, **315**, 5:1–5:19, ISSN 1868-8969.

Krenn, P. J., P. Oja and S. Titze (2014) Route choices of transport bicyclists: a comparison of actually used and shortest routes, *International Journal of Behavioral Nutrition and Physical Activity*, **11** (1) 31, ISSN 1479-5868.

Landeshauptstadt München (2019) Geodaten - Nutzung, 2019.

Loder, A., F. Cantner, L. Adenaw, N. Nachtigall, D. Ziegler, F. Gotzler, M. B. Siewert, S. Wurster, S. Goerg, M. Lienkamp and K. Bogenberger (2024) Observing Germany's nationwide public transport fare policy experiment "9-Euro-Ticket" – Empirical findings from a panel study, *Case Studies on Transport Policy*, **15**, 101148, March 2024, ISSN 2213624X.

Manley, E., S. Orr and T. Cheng (2015) A heuristic model of bounded route choice in urban areas, *Transportation Research Part C: Emerging Technologies*, **56**, 195–209, ISSN 0968090X.

Martin, H., H. Becker, D. Bucher, D. Jonietz, M. Raubal and K. W. Axhausen (2019) Begleitstudie SBB Green Class - Abschlussbericht, 56 p.

Meister, A., M. Felder, B. Schmid and K. W. Axhausen (2023) Route choice modeling for cyclists on urban networks, *Transportation Research Part A: Policy and Practice*, **173**, 103723, July 2023, ISSN 09658564.

Oja, P., S. Titze, A. Bauman, B. de Geus, P. Krenn, B. Reger-Nash and T. Kohlberger (2011) Health benefits of cycling: a systematic review, *Scandinavian Journal of Medicine and Science in Sports*, **21** (4) 496–509, April 2011, ISSN 1600-0838.

Pappalardo, L., E. Manley, V. Sekara and L. Alessandretti (2023) Future directions in human mobility science, *Nature Computational Science*, July 2023, ISSN 2662-8457.

Park, Y. and G. Akar (2019) Why do bicyclists take detours? A multilevel regression model using smartphone GPS data, *Journal of Transport Geography*, **74**, 191–200, ISSN 09666923.

Skov-Petersen, H., B. Barkow, T. Lundhede and J. B. Jacobsen (2018) How do cyclists make their way? - A GPS-based revealed preference study in Copenhagen, *International Journal of Geographical Information Science*, **32** (7) 1469–1484, July 2018, ISSN 1365-8816, 1362-3087.

Skupin, A. (2008) Visualizing Human Movement in Attribute Space, in P. Agarwal and A. Skupin (eds.) *Self-Organising Maps*, 1 edn., 121–135, Wiley, ISBN 978-0-470-02167-5 978-0-470-02169-9.

Sultan, J., G. Ben-Haim, J. Haunert and S. Dalyot (2017) Extracting spatial patterns

in bicycle routes from crowdsourced data, *Transactions in GIS*, **21** (6) 1321–1340, December 2017, ISSN 1361-1682, 1467-9671.

Teimouri, F. and K.-F. Richter (2022) Abstracting routes to their route-defining locations, *Computers, Environment and Urban Systems*, **91**, 101732, ISSN 01989715.

Teimouri, F. and K.-F. Richter (2025) Enhancing wayfinding and route learning: a human-centred study of the route-defining locations algorithm, *Behaviour & Information Technology*, **44** (1) 44–60, ISSN 0144-929X, 1362-3001.

Teimouri, F., K.-F. Richter and H. H. Hochmair (2023) Analysis of route choice based on path characteristics using Geolife GPS trajectories, *Journal of Location Based Services*, 1–27, ISSN 1748-9725, 1748-9733.

Wiener, J. M., T. Tenbrik, J. Henschel and C. Holscher (2008) Situated and prospective path planning: Route choice in an urban environment.

Willis, D. P., K. Manaugh and A. El-Geneidy (2015) Cycling Under Influence: Summarizing the Influence of Perceptions, Attitudes, Habits, and Social Environments on Cycling for Transportation, *International Journal of Sustainable Transportation*, **9** (8) 565–579, November 2015, ISSN 1556-8318, 1556-8334.

Zheng, Y. (2015) zheng: An Overview, *ACM Transactions on Intelligent Systems and Technology*, **6** (3) 1–41, ISSN 2157-6904, 2157-6912.

Zürich, S. (2021) Https://data.stadt-zuerich.ch/dataset/geo_signalisierte_geschwindigkeiten.

A Descriptive network statistics

Table 2: Descriptive network statistics

	Central Munich (64 km^2, 2022)				Zurich region (400 km^2, 2017)			
Attribute	Mean	Std	Min	Max	Mean	Std	Min	Max
Access by car	0.838	0.368	0.0	1.000	0.666	0.472	0.0	1.000
Access by foot	0.997	0.056	0.0	1.000	0.978	0.146	0.0	1.000
Advisory lane	0.031	0.173	0.0	1.000	0.027	0.161	0.0	1.000
Bicycle Road	0.015	0.123	0.0	1.000	0.000	0.000	0.0	0.000
Bicycle path surface	12.600	8.269	0.0	20.000	4.984	7.609	0.0	20.000
Bicycle path width	1.729	1.416	0.7	7.906	18.000	0.000	18.0	18.000
Exclusive lane	0.004	0.060	0.0	1.000	0.000	0.004	0.0	1.000
Foot_and_cycle_path	0.079	0.270	0.0	1.000	0.024	0.153	0.0	1.000
Crossing	0.002	0.049	0.0	1.000	0.000	0.004	0.0	1.000
Gradient	0.017	0.040	0.0	0.815	0.052	0.118	0.0	3.658
Share of green areas	0.239	0.368	0.0	1.000	0.173	0.353	0.0	1.000
Stret lighting	0.540	0.498	0.0	1.000	0.017	0.130	0.0	1.000
Parking (left)	0.212	0.607	-1.0	2.000	0.000	0.027	-1.0	2.000
Parking (right)	0.243	0.646	-1.0	2.000	0.000	0.032	-1.0	2.000
Share of retail areas	0.115	0.287	0.0	1.000	0.014	0.103	0.0	1.000
Road hierarchy	5.472	1.366	0.0	9.500	4.235	3.021	0.0	9.625
Intersection hierarchy	5.217	1.816	0.0	9.500	3.901	3.198	0.0	9.625
Number of lanes	2.290	0.846	1.0	7.000	1.139	0.603	0.0	5.000
Speed limit	35.435	10.200	4.0	60.000	39.020	15.466	0.0	120.000
One-way	0.114	0.318	0.0	1.000	0.049	0.217	0.0	1.000
Number of PT routes	0.170	1.841	0.0	139.000	0.116	1.374	0.0	55.000
One-direction_cycle-path	0.119	0.323	0.0	1.000	0.004	0.063	0.0	1.000
Pedestrian_street	0.004	0.061	0.0	1.000	0.001	0.027	0.0	1.000
Track_or_lane	0.001	0.032	0.0	1.000	0.001	0.023	0.0	1.000
Two-direction_cycle-path	0.014	0.117	0.0	1.000	0.020	0.141	0.0	1.000

B Additional information

Number of samples per mask in Figure 1:

Table 3: Number of samples per mask

Mask	Zurich	Munich
Total Paths	452	1000
Distance		
1–2 km	159	339
2–3 km	48	213
3–4 km	38	149
4–5 km	39	93
Frequency		
Repeat	115	89
Non-repeat	337	911
Purpose		
Work	169	140
Leisure	64	180

The distribution of the normalized edge costs is shown in Figure 2

Figure 2: Distribution of the normalized edge costs.